

Chemical Sensors Based on Quantum Cascade Lasers

Anatoliy A. Kosterev and Frank K. Tittel, *Fellow, IEEE*

Invited Paper

Abstract—There is an increasing need in many chemical sensing applications ranging from industrial process control to environmental science and medical diagnostics for fast, sensitive, and selective gas detection based on laser spectroscopy. The recent availability of novel pulsed and CW quantum cascade distributed feedback (QC-DFB) lasers as mid-infrared spectroscopic sources address this need. A number of spectroscopic techniques have been demonstrated worldwide by several groups. For example, the authors have employed QC-DFB lasers for the monitoring and quantification of several trace gases and isotopic species in ambient air at ppmv and ppbv levels by means of direct absorption, wavelength modulation, and cavity enhanced and cavity ringdown spectroscopy.

Index Terms—Infrared spectroscopy, quantum cascade lasers, trace gas detection.

I. INTRODUCTION

INFRARED laser absorption spectroscopy is an extremely effective tool for the detection of molecular trace gases. The demonstrated sensitivity of this technique is at the parts per trillion level. The usefulness of the laser spectroscopy approach is limited by the availability of convenient tunable sources in the region of fundamental vibrational absorption bands from 3 to 20 μm . Real world applications require the laser source to be compact, highly efficient, and preferably working at room temperature. The existing options include cryogenically cooled lead salt diode lasers [1], [2] and coherent sources based on difference frequency generation (DFG) [3]. Sensors based upon lead salt diode lasers are typically large in size and require consumables because these diodes operate at temperatures of <90 K. DFG-based sources (especially PPLN based) have been shown to be very robust, compact, and suitable for many atmospheric monitoring applications. However, DFG sources generate inherently low IR power, and spectral coverage of PPLN based devices is limited to wavelengths shorter than 5 μm , which restricts the number of detectable molecules.

The advance of quantum cascade (QC) lasers fabricated by band structure engineering offers an attractive new option for

IR absorption spectroscopy. The most technologically developed system to date is based on intersubband transitions (type-I QC) in InGaAs–InAlAs heterostructures [4]. QC lasers are usually fabricated as a single-mode waveguide, and a distributed feedback (DFB) structure can be implemented by etching the top cladding layer. QC-DFB lasers are of particular interest to gas-sensing applications, because they emit single-frequency radiation that is suitable for high-resolution spectroscopy. Other QC systems such as type-I GaAs–AlGaAs [5] and type-II (interband) lasers [6], [7] have not yet reached the level of robustness required by real-world chemical sensing applications.

Compared to Pb-salt diode lasers, QC-DFB lasers allow the realization of compact narrow-linewidth mid-IR sources combining single-frequency operation and substantially higher powers (tens of milliwatts) at mid-IR wavelengths (3.5 to 24 μm). The large wavelength coverage available with QC lasers allows numerous molecular trace gas species to be monitored. QC lasers are the only semiconductor lasers able to emit mid-IR radiation at room temperature and above [4], [8]. The higher power of QC lasers permits the use of advanced detection techniques that significantly improve the SNR of trace gas spectra and decrease the sensor size. For example, in cavity enhanced spectroscopy (CES) and cavity ringdown spectroscopy (CRDS) an effective absorption pathlength of hundreds of meters can be obtained in a laptop-size device [9], [10]. Recent work with QC-DFB lasers described in this review has demonstrated the usefulness of these devices for sensitive, highly selective, real-time trace gas concentration measurements based on absorption spectroscopy with sensitivities of several parts per billion by volume (ppbv).

Unipolar QC-DFB lasers are inherently capable of operating at high temperature of the active region, considerably exceeding room temperature. However, the power dissipation in these devices is higher than in diode lasers and often surpasses 10 W. In CW operation, the temperature of the active region is >100 K higher than that of the substrate temperature. Until recently, this has made it impossible to realize CW operation of QC lasers without cryogenic cooling. The latest technological progress in QC laser engineering resulted in devices that can be operated in a CW mode with thermoelectric temperature control [11], [12].

CW operation of QC-DFB lasers can be employed presently to achieve the best detection sensitivity when cryogenic consumables and a large instrumental footprint are not primary practical issues. For example, a CW QC-DFB laser operated at 82 K in a liquid nitrogen Dewar was used in an airborne sensor for atmospheric detection of CH_4 and N_2O [13]. The

Manuscript received November 30, 2001; revised February 28, 2002. This work was supported by the National Aeronautics and Space Administration, the Institute for Space Systems Operations, University of Houston, the Texas Advanced Technology Program, the National Science Foundation, and the Welch Foundation.

The authors are with Rice Quantum Institute, Rice University, Houston, TX 77251-1892 USA (e-mail: akoster@rice.edu).

Publisher Item Identifier S 0018-9197(02)05026-1.

CW QC-DFB laser linewidth is as narrow as 1–3 MHz when a ripple-free current source is applied [14]–[16] and a few kilohertz when a frequency stabilization feedback loop is employed [17]. In fact, all the spectroscopic methods developed for mid-IR Pb-salt diode lasers including fast frequency scanning with modulated injection current can be applied with the added advantage of reliable and reproducible single-frequency operation and high power up to 150 mW [4].

A solution for noncryogenic QC-DFB laser-based spectroscopy is to apply very short (5–50 ns) pulses of the pump current at a low duty cycle, typically <1%. In pulsed operation the minimum QC-DFB laser linewidth is typically ~ 250 MHz due to the frequency chirp related to the fast heating of the active area during the pump current pulse.¹ Such linewidth is acceptable for most gas sensing applications. Concentration measurements in gases are usually performed at pressures of ~ 100 torr and above, when pressure broadened absorption lines are wider than >500 MHz. At this time the pulsed mode of QC-DFB laser operation has a clear advantage for mobile sensors because it eliminates the need for cryogenic cooling.

II. CHEMICAL SENSING BASED ON DIRECT IR ABSORPTION SPECTROSCOPY

A. Detection of Trace Gases With CW QC-DFB Lasers

Gas sensing with a CW QC-DFB laser was first reported in [18]. The laser was scanned via a sawtooth current ramp (5–11 kHz) and the absorbance of the sample was measured directly. It was possible to sweep the laser rapidly over a frequency range of up to 2.5 cm^{-1} . Absorption spectra of pure NO and NH₃ gases at low pressure were acquired at 5.2 and 8.5 μm , respectively.

The direct absorption approach with CW QC-DFB lasers was further developed in [19] and the first successful application of a single-frequency QC-DFB laser to the analysis of trace gases in ambient air was reported in [20]. The schematic of the CW QC-DFB laser based gas sensor used in [20] is shown in Fig. 1. In these experiments, a QC-DFB laser designed for CW operation at cryogenic temperatures in the 7.9- μm spectral region was used. The laser was placed in a liquid nitrogen Dewar, and no active temperature stabilization was applied. To avoid fast boil-off of liquid nitrogen and related frequency and alignment drifts, the laser was operated at a reduced duty cycle (typically 10% to 25%). Current was supplied in pulses of 120–235- μs duration at a 0.8–1-kHz repetition rate. The lasing characteristics under such long pump current pulses are essentially the same as in real CW operation, because the temperature of the laser active region reaches equilibrium on a nanosecond time scale. Each current pulse resulted in a frequency scan covering $\sim 2\text{ cm}^{-1}$. Absorption in air was detected in a 100-m multipass cell at a reduced pressure of 20–40 torr. A “zero-air” background subtraction technique [21] was used in order to suppress the influence of interfering effects. Spectra of ambient air and pollutant-free “zero air” were acquired alternatively. The zero-air signal (as a function of a datapoint number) was subtracted from the ambient air sample signal and normalized to the zero-air signal.

¹We recently observed a linewidth of 150 MHz in pulsed, near room-temperature operation of a $\lambda = 15.5\text{ }\mu\text{m}$ QC-DFB laser from Alpes Lasers.

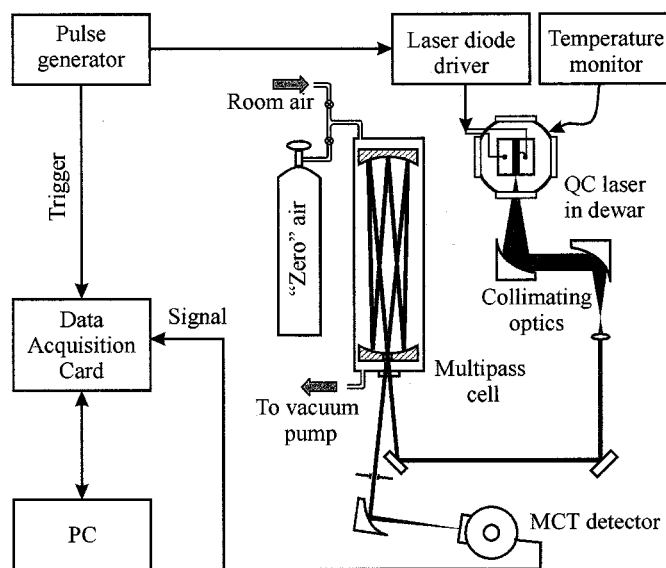


Fig. 1. Schematic of a CW QC-DFB-based gas sensor [20].

This procedure resulted in an absorption spectrum of the ambient air sample. In most measurements, synthetic air with an addition of 5% CO₂ was used as so-called “zero-air” gas. The resulting weak CO₂ lines of apparently negative absorption in the acquired spectra aided in the spectral calibration of wavelength scans.

A typical absorption spectrum of ambient air is shown in Fig. 2, which was obtained with a QC-DFB laser using the setup depicted in Fig. 1. Four strong methane lines, two strong nitrous oxide lines, and several water lines corresponding to different isotopic species fall into the spectral range covered by a frequency scan of 2 cm^{-1} centered at 1260 cm^{-1} . The spectrum depicted is the result of averaging over 6000 individual scans for both ambient air and zero-air. The acquisition and averaging of 6000 200- μs -long scans with 50 megasamples per second at 1-kHz repetition rate required ~ 30 s. Optimized software could permit faster data acquisition by utilizing a larger fraction of the frequency scans.

The CH₄ and N₂O concentration levels in the ambient air were determined by fitting the envelopes of the stronger absorption lines with a Voigt function. The area under a fitting curve was compared with that predicted from the HITRAN database. To estimate the sensitivity of this gas sensor, a part of the spectrum containing no absorption lines was selected and the fitting procedure was applied to find an absorption feature similar to a CH₄ absorption line. The typical peak absorbance of such a feature did not exceed $\pm 3.5 \times 10^{-5}$, or 8×10^{-5} fractional absorption. For the strongest absorption lines in this part of the IR spectrum, a detection limit of 2.5 ppbv for CH₄ and 1.0 ppbv for N₂O was established.

Detection of more complex organic molecules with congested unresolved ro-vibrational spectra sets a specific challenge to QC-DFB laser-based chemical sensors. Traditionally the spectral recognition of such species is performed by acquiring medium-resolution absorption spectra in a wide spectral region (thousands of wavenumbers) and then identifying absorption bands rather than isolated lines. This approach

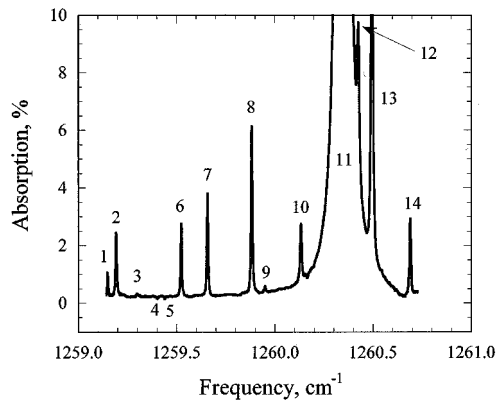


Fig. 2. An example of an absorption spectrum of room air obtained with a gas sensor depicted in Fig. 1. The assignment of the stronger spectral lines is shown: H_2^{16}O —1, 11, 13; N_2O —2, 3, 10; CH_4 —6, 7, 8, 14; H_2^{18}O —9; HDO —12; and CO_2 in the reference zero-air that appears as a negative absorption—4, 5.

cannot be realized with QC-DFB lasers because of their limited tunability. The laser frequency usually changes with the heat sink temperature with a coefficient of 0.05 to 0.15 cm^{-1}/K . The maximum demonstrated spectral range covered by a single-frequency QC-DFB laser is $\sim 30 \text{ cm}^{-1}$, achieved in pulsed operation when the heat sink temperature varied from 50 to 300 K [4]. However, such a wide spectral coverage can be realized only for selected devices. One of the limiting factors is a mismatch between the active region peak-gain and the DFB structure mode, due to their different temperature dependence [22]. Another limitation for current-tuning of a CW laser is that at a certain current level higher order transverse modes can reach a lasing threshold, and also the maximum current for a particular laser chip must not be exceeded. In practice, the tunability of a QC-DFB laser in a chemical sensor is usually limited to 1–3 cm^{-1} .

The feasibility of detecting and quantifying volatile organic compounds was explored in [20] using ethanol ($\text{C}_2\text{H}_5\text{OH}$) as an example. Fig. 3 shows the ethanol vapor absorption spectra (for ethanol at 1 torr partial pressure with ambient air added to a total pressure of 36.6 torr) acquired with the QC-DFB laser in a 0.43-m-long gas cell. Air was added to provide the same pressure broadening conditions as in successive multipass cell experiments; absorption by the air components was negligibly small compared to absorption by the ethanol vapor. The rovibrational structure is reasonably well resolved, unlike in the C—H and O—H stretch spectral region ($\lambda \sim 3 \mu\text{m}$). This is due to the smaller Doppler width and the much smaller density of vibrational states at 1200 cm^{-1} compared to 3000 cm^{-1} . The resolved spectral features (they do not represent individual rovibrational transitions but clusters of absorption lines) clearly distinguish the absorption of ethanol from other species. However, the high density of the unresolved pressure-broadened spectral lines makes the technique of individual line fitting with a Voigt profile (local approach) inapplicable. Instead, some kind of global approach should be used in order to take advantage of the whole spectral fingerprint. The technique used in [20] is principally based on finding the correlation between previously acquired *reference* spectra and a sample spectrum (*test* spectrum) under the same line-broadening conditions (i.e., if the air

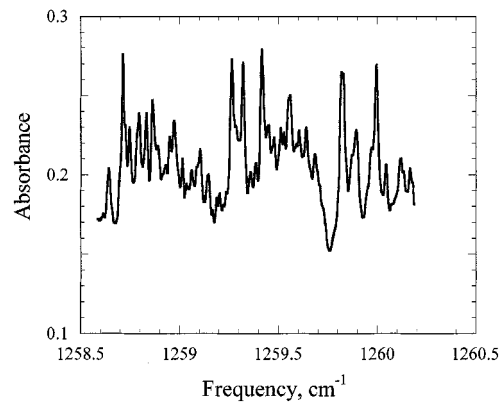


Fig. 3. Ethanol absorption spectra obtained in a 0.43 m long gas cell. Partial pressure of ethanol is 1 torr, room air added to a total pressure of 36.6 torr.

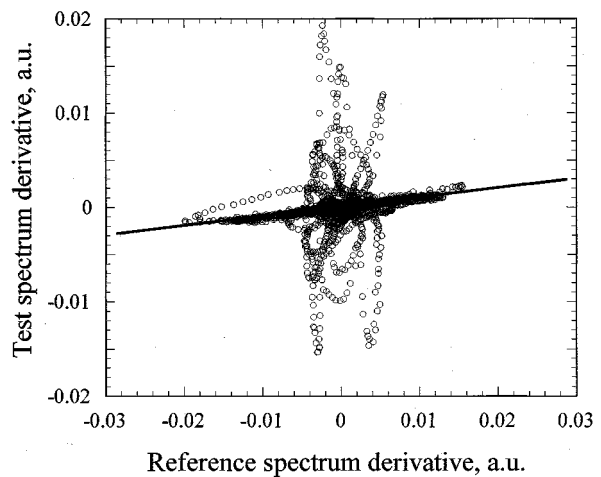


Fig. 4. Test spectrum derivative as a function of the reference spectrum derivative [20]. The test sample of room air is taken 7 min after evaporating a few drops of ethanol near the multipass cell. The fitted line slope yields $k = 9.82 \times 10^{-2}$, corresponding to an ethanol concentration of 12.1 ppm.

pressure and temperature are the same). Each data point value y_i from the test spectrum was plotted as a function of the corresponding reference spectrum point x_i (a numerical derivative of both spectra was taken beforehand, see [20] for details), and the slope of the best fit $y = kx$ [1-D linear regression (1DLR)] yielded the ethanol concentration in the air sample as shown in Fig. 4. The loops of outlying points occur because of strong absorption lines of H_2O , N_2O and CH_4 . Spectra of all these molecules are well known, and therefore a 1DLR approach was generalized to the multidimensional linear regression (MLR) in order to acquire the concentrations of all the species in a single fitting procedure. The test spectrum was considered as a linear combination of four reference spectra of the absorbing species

$$y_i = \sum_{k=1}^4 a_k x_{ki} \quad (1)$$

where y_i is the i th datapoint of the test spectrum, a_k gives the contribution of each absorbing component to the resulting spectrum, $k = 1..4$ corresponds to $\text{C}_2\text{H}_5\text{OH}$, CH_4 , N_2O and H_2O , respectively, and x_{ik} is the intensity of the k th reference spectrum at the frequency of the i th datapoint. The resulting con-

concentrations were found to be mutually consistent and in agreement with the 1DLR (ethanol concentration) and concentrations of H_2O , N_2O , and CH_4 extracted from the same spectra by the conventional single-line fitting approach. Hence, high-resolution IR absorption data acquired in a limited $1\text{--}3\text{ cm}^{-1}$ range with a QC-DFB laser can be successfully used for quantification of multiple trace gas components, including complex organic compounds.

Non-DFB multimode QC lasers (Fabry–Pérot devices) may find application in differential absorption lidar (DIAL) systems [23]. There exists a wide-ranging interest in extending DIAL-based chemical sensing from the detection and quantification of major species to the characterization of dilute contaminants, e.g., organic chemical vapors that do not possess spectrally resolved vibrational transitions. In general, the $8\text{--}12\text{-}\mu\text{m}$ wavelength spectral region is the most desirable wavelength range for performing sensitive, selective detection of organic species. Several QC lasers could be simultaneously used in a DIAL system to probe the broad absorption features at selected wavelengths. A pseudorandom code modulation is proposed to distinguish signals produced by different lasers [23].

B. Detection of Trace Gases With Pulsed QC-DFB Lasers

One of the most attractive features of QC lasers is their ability to be operated at quasi-room temperature. This option is presently restricted to pulsed QC-DFB devices, which results in a number of specific performance issues. The most fundamental of them are reduced average power (peak power is essentially the same as in a CW mode, but the duty cycle is $<1\%$) and laser line broadening caused by frequency chirping during the pump current pulse. The first work on spectroscopic chemical sensing with a pulsed QC-DFB laser was reported in 1998 [24], preceding the first CW QC-DFB laser-based publication [18]. The authors introduced a technique of fast-tuning the optical frequency of the laser pulses by applying a subthreshold current (STC) ramp. Wavelength modulation spectra of diluted N_2O and CH_4 samples were acquired near $\lambda = 8\text{ }\mu\text{m}$. The laser was excited by a 1-MHz train of 11-ns-wide current pulses. The laser linewidth was estimated to be 720 MHz. Detection was performed with a slow HgCdTe detector in essentially the same manner as in CW experiments. A similar approach to detection was used in [25] and referred to as “quasi-CW.”

An alternative approach to data acquisition with pulsed QC-DFB lasers is to use a fast detector and measure the peak power or integrated energy of every pulse with gated electronics. In this mode of measurement, the detected signal is much higher than the detector noise and does not depend on the repetition rate. Time-gating permits suppression of the scattered light that occurs earlier or later than the informative signal. This approach was utilized in the first successful application of a pulsed QC-DFB laser to the trace gas detection in ambient air [26].

A schematic of the pulsed QC-DFB laser based gas sensor configuration used in [26] is shown in Fig. 5. A QC-DFB laser designed for pulsed near-room temperature operation at $\sim 8\text{ }\mu\text{m}$ was mounted on a three-stage thermoelectric cooling module inside a compact evacuated housing ($75 \times 75 \times 75\text{ mm}^3$). The temperature of the QC-DFB laser could be varied from $-40\text{ }^\circ\text{C}$

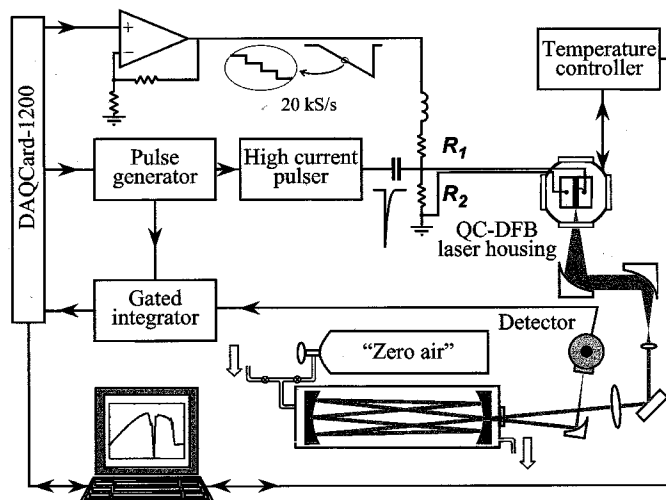


Fig. 5. Schematic of a gas sensor based on a pulsed QC-DFB laser [26].

to above room temperature. In practice, the laser temperature was usually kept below $+6\text{ }^\circ\text{C}$ because of a rapid decrease in laser power, an increase of threshold current, and the appearance of mode instabilities at higher temperatures. The optical configuration of this sensor was similar to that used for CW QC laser-based trace gas detection [20]. The laser was pumped by 5-ns-long current pulses at a 20-kHz repetition rate. Such short pulses were shown to ensure the minimum linewidth for this laser, namely 290 MHz. In this work, a novel approach to the wavelength manipulation of a QC-DFB laser pulses was used. An STC waveform was not supplied as a ramp from a function generator but instead was synthesized by a computer-controlled digital–analog converter. The timing of consecutive STC updates was synchronized to the pump current pulses. In this manner, the relative wavelength of each laser pulse in a wavelength scan was independently and unambiguously controlled. Computer control adds flexibility to the device architecture, providing arbitrary modulation waveforms that can be applied to the QC laser. The absolute wavelength position of a scan is determined by the laser substrate temperature.

The laser pulses were detected using a liquid nitrogen cooled photovoltaic HgCdTe detector (which, if necessary, can be replaced by a thermoelectrically cooled detector). The detector signal was measured using a gated integrator and a 12-bit data acquisition card connected to a laptop computer. An integration window of 15 ns was set to integrate the signal at the peak of the $\sim 35\text{-ns}$ FWHM detector response. The useful signal was separated in time from any interfering scattered light due to a 330-ns delay of the laser pulse in the multipass cell. For data analysis a linear regression technique similar to the one used in [20] for ethanol detection was employed. This technique enables rapid calculations and takes into account a nonnegligible asymmetric laser line shape. The flexibility provided by the new digital frequency control approach was utilized for linearization of the wavelength scan and for a novel scheme of wavelength modulation spectroscopy in an independent run of measurements. The sensor was used to measure CH_4 , N_2O and HDO concentrations in ambient air, and a precision of 9, 4, and 120 ppbv was achieved for each of these species, respectively.

A compact mobile ammonia sensor based on a thermoelectrically cooled pulsed QC-DFB laser operating at $\sim 10 \mu\text{m}$ was described in [27]. High-sensitivity detection of NH_3 is of interest in the control of deNO_x chemistry, industrial safety, and medical diagnostics of kidney related diseases. The optical configuration of this sensor was similar to that described in [26], but the multipass cell was replaced with a simple 50-cm-long double pass gas cell, and no zero-air was employed. The laser housing was improved by replacing the previous beam-shaping optical system consisting of two off-axis parabolic mirrors and a lens with a single aspheric lens. The laser was scanned over two absorption lines of the NH_3 fundamental ν_2 band. The sensor was completely automated and only required the liquid N_2 Dewar of the detector to be refilled every 12 h. This sensor was applied to measurements at NASA-Johnson Space Center, Houston, TX, to continuous long-term monitoring of NH_3 concentration levels present in bioreactor vent gases. A sensitivity of better than 0.3 ppmv was estimated which was sufficient to quantify expected ammonia levels of 1–10 ppmv.

A further improvement of the pulsed QC-DFB based sensor configuration was reported in [28]. The laser beam was split into two channels, one being used to probe the gas absorption and the other as a reference to measure the laser pulse energy. The subsequent normalization eliminated pulse-to-pulse energy fluctuations as an error source, which was the predominant cause in [27]. Such an automated sensor was used for continuous monitoring of CO in ambient air detected by its R(3) absorption line at 2158.300 cm^{-1} ($\lambda \sim 4.6 \mu\text{m}$). A noise-equivalent detection limit of 12 ppbv was experimentally demonstrated with a 1-m optical pathlength. This sensitivity corresponds to a standard error in fractional absorbance of 3×10^{-5} .

The design and performance of an optical mid-IR CO sensor intended for continuous *in vitro* monitoring of cell culture activity at ambient atmospheric pressure is presented in [29]. The typical production rate of CO, for example from vascular smooth muscle cells, is 1 to 10 pmol/min/ 10^7 cells. Instrumentation for *in vitro* measurement of gas production should have sensitivities on the parts per billion (ppbv) level so that the dynamics of gas production can be followed with laboratory-scale cell sample populations. Because of the low production rate from biological tissues, measurements of CO concentrations have been limited to gas chromatography and radioisotope counting techniques. Although these methods are highly sensitive, they cannot measure CO directly, requiring several time-consuming intermediate steps (~ 15 min), and may be affected by interferences from water, oxygen, and carbon dioxide. The sensor described in [29] used the same QC-DFB laser at $\lambda \sim 4.6 \mu\text{m}$ [28] as a spectroscopic source and a two-channel configuration with a 1-m optical pathlength inside a cell culture container. All the measurements were carried out at atmospheric pressure, and hence it was not possible to periodically acquire a baseline with an evacuated sample container. In order to keep the baseline (which included weak unwanted interference fringes from optical elements) stable during multihour measurements, the slow drifts of the laser frequency were actively compensated by computer-controlled corrections to the STC. A constant CO production rate of 44 ppbv/h was observed, taking into account the 0.5-L volume

of the cell culture container. This corresponds to a net CO production rate of $0.9 \text{ nmol}/10^7 \text{ cells/h}$, which is in agreement with previous measurements obtained with similar cells and treatment regimes [30].

Multimode pulsed Fabry–Pérot QC lasers can be used in analytical applications that do not require or would not benefit from high spectral resolution. One example is a spectroscopic analysis of liquids, where the spectral lines are broad. Such an application was demonstrated in [31] to quantify phosphate in Diet Coke samples. A fiber-coupled injection cell with a pathlength of $\sim 100 \mu\text{m}$ in the aqueous sample was used. The results were in good agreement with the values found by ion chromatography.

III. SENSORS USING A HIGH-FINESSE OPTICAL CAVITY

Sensitive laser absorption spectroscopy often requires a long effective pathlength of the probing laser beam in media being analyzed. Traditionally, this requirement is satisfied using an optical multipass cell. Such an approach has a number of shortcomings, especially for compact gas sensors. Multipass cells tend to be bulky. For example, a commercial 100-m pathlength cell (New Focus Model 5612, now offered by Aerodyne, Inc.) has a volume of 3.5 L. Such gas absorption cells also require costly large-aperture mirrors sometimes with aspheric surfaces. Light scattering or beam clipping on input apertures create interference fringes that limit sensitivity. An alternative way to obtain a long optical path is to make the light bounce along the same path between two parallel ultralow-loss dielectric mirrors. In this case, the effective optical pathlength L is given by the expression $L = l/(1 - R)$, where l is the mirror spacing and R is the reflection coefficient of each mirror. An effective optical pathlength of several kilometers can be obtained in a very small volume $V = Sl$, where S is the laser beam cross-sectional area. The light leaking out of such an optical cavity can be used to characterize the absorption of the intracavity medium. Presently a variety of techniques exists to perform high-sensitivity absorption spectroscopy in a high-finesse optical cavity (see, for example, [10]). One of the most advanced is the so-called “Noise-Immune Cavity-Enhanced Optical Heterodyne Spectroscopy” (NICE-OHMS) technique [32]. It has the potential to provide shot-noise-limited sensitivity with an effective pathlength determined by the cavity ringdown time. The first implementations of this technique in combination with a QC-DFB laser is reported in [33]. However, this approach is technically sophisticated and probably not suitable for most practical chemical-sensing applications. We shall consider two other, simpler methods in more details.

A. Cavity Ringdown Spectroscopy With QC-DFB Lasers

Cavity ringdown spectroscopy (CRDS) was first introduced in [9]. This work was carried out with a high-power pulsed laser. A short light pulse injected into a high-finesse optical cavity produces a sequence of pulses leaking out through one of the mirrors (cavity ringdown) due to consecutive reflections. The intensity of pulses in such a pulse train decays exponentially with a time constant

$$\tau = \frac{l}{c} \cdot \frac{1}{\alpha l - \ln R} \quad (1)$$

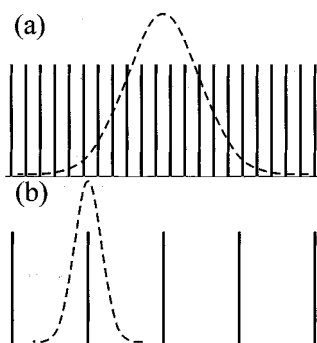


Fig. 6. Two situations of laser radiation filtering by the optical cavity (idealized one-dimensional consideration). (a) The laser linewidth is much broader than the cavity mode spacing. In this case, the cavity throughput does not depend on the laser linewidth but is solely defined by the cavity finesse. (b) The laser linewidth is less than the cavity mode spacing. The cavity throughput is determined by the ratio of the cavity mode width to the laser linewidth.

where α is the absorption coefficient of the intracavity medium and R is the mirror reflectivity. This technique is simple and immune to laser power fluctuations. Unfortunately, it cannot be directly utilized with pulsed QC lasers. The energy of the first pulse in the ringdown sequence is $(1 - R)^2$ times less than the exciting laser pulse. The mirrors for CRDS experiments typically have a reflectivity $R > 99.95\%$. This makes the measurements with ~ 1 -nJ IR pulses (available energy $E \sim 100$ mW \times 10 ns) practically impossible.

The approach described in [9] corresponds to the frequency-domain picture shown in Fig. 6(a). The laser line represented by the dashed curve is much broader than the cavity mode spacing $\Omega = c/2l$. The cavity throughput can be made much higher if the laser linewidth $\Delta\nu_L \ll \Omega$. This condition can be satisfied if a narrow-line cw laser is used. When the laser frequency coincides with one of the cavity modes as shown in Fig. 6(b), the cavity throughput is approximately $T = \Delta\nu_C/\Delta\nu_L$, where $\Delta\nu_C$ is the spectral width of the cavity mode. After the cavity is filled with radiation, the laser emission can be interrupted and the ringdown decay measured in the same manner as is done with a pulsed laser. This CW modification of CRDS was introduced in [34].

The first work on CRDS measurements with a QC-DFB laser was published in 2000 [35]. The authors used a CW laser generating 16 mW at $\lambda = 8.5$ μm . The measured ringdown time of the empty three-mirror cavity was 0.93 μs . An acoustooptic modulator was used to interrupt the cavity injection for ringdown time measurements. The system was tested on diluted ammonia mixtures, and a noise-equivalent sensitivity of 0.25 ppbv achieved. An estimated 1.0×10^{-9} cm^{-1} detectable absorbance limit was reported.

In [14], a spectroscopic gas sensor for NO detection based on a cavity ringdown technique is described. NO is the major oxide of nitrogen formed during high-temperature combustion as well as an important nitrogen-containing species in the atmosphere (NO is a precursor of smog and acid rain). NO is also involved in a number of vital physiological processes, and its detection in human breath has potential applications (e.g., as a marker for diseases like asthma or inflammatory processes) in noninvasive medical diagnostics. A CW QC-DFB laser operating at 5.2 μm was used as a tunable single-frequency light source. The tech-

nique used in [14] was similar to the scheme first reported by Romanini *et al.* [34] and later applied in [35] for CRDS with a CW QC-DFB laser. It consists of the following features.

- 1) The laser frequency is slowly scanned across the absorption line of interest.
- 2) One of the cavity mirrors is dithered back and forth to ensure periodic, random coincidences of the laser frequency with a cavity mode.
- 3) Once such a resonance occurs and the cavity is filled, the laser beam entering the cavity is abruptly interrupted or set off-resonance, and the decay rate of the exiting light is measured.

From (1), the absorption coefficient can be determined as

$$\alpha = \frac{1}{c} \left(\frac{1}{\tau} - \frac{1}{\tau_{\text{empty}}} \right) \quad (2)$$

where τ_{empty} is the decay constant of the cavity when evacuated.

The sensor schematic is shown in Fig. 7. It depicts a simpler design than the first CRDS experiment with a QC-DFB laser described in [35]. In that work, a variable temperature cryostat for laser frequency tuning was used with the inherent complexity and additional cost of an acoustooptic modulator to interrupt the QC laser beam. In our work [14], both frequency tuning and the laser emission interruption were realized by manipulation of the QC laser pump current. No active temperature control was applied to the QC-DFB laser located in a liquid nitrogen optical cryostat. The laser current was supplied by a low-noise home-built current source and monitored using the 0.5- Ω resistor denoted by r_1 in Fig. 1. The laser frequency was tunable from 1922.9 to 1920.8 cm^{-1} when the pump current changed from 300 (lasing threshold) to 660 mA. At higher current levels, the laser emission was multimode. The tuning range permitted NO detection by accessing absorption lines at 1921.599 and 1921.601 cm^{-1} [R(13.5) [R(13.5) components of the fundamental absorption band]. Absorption lines of water vapor and CO_2 were also observed. The $l = 37$ -cm long, linear high-finesse optical cavity was formed by two concave mirrors with a 6-m radius of curvature. The measured ringdown time of the evacuated cavity was $\tau \approx 3.5$ μs , corresponding to $\Delta\nu_C \approx 45$ kHz. The laser linewidth was estimated to be $\Delta\nu_L = 3$ MHz.

When a certain level of the detector signal was reached signaling that a TEM_{00} cavity mode is coupled to the laser, a triggering circuit (TC) opened a metal-oxide semiconductor field-effect transistor (MOSFET) to shunt the laser current, thereby reducing it to a subthreshold value. At the same time, the TC triggered an analog-digital converter, and the detector signal showing the cavity ringdown was digitized for ~ 30 μs and stored in computer memory. The MOSFET was kept open for 35 μs , so that the laser radiation would not interfere with measurements of the cavity decay constant. This triggering-and-acquisition process was repeated and consecutive ringdown transients were stacked in the A/D memory until a desired number of transients was acquired. The results were post-processed to fit each transient with an exponential decay function yielding a ringdown time τ . An inverse ringdown time plotted as a function of the laser current provides the absorption spectrum. An example of the NO absorption in a mixture with

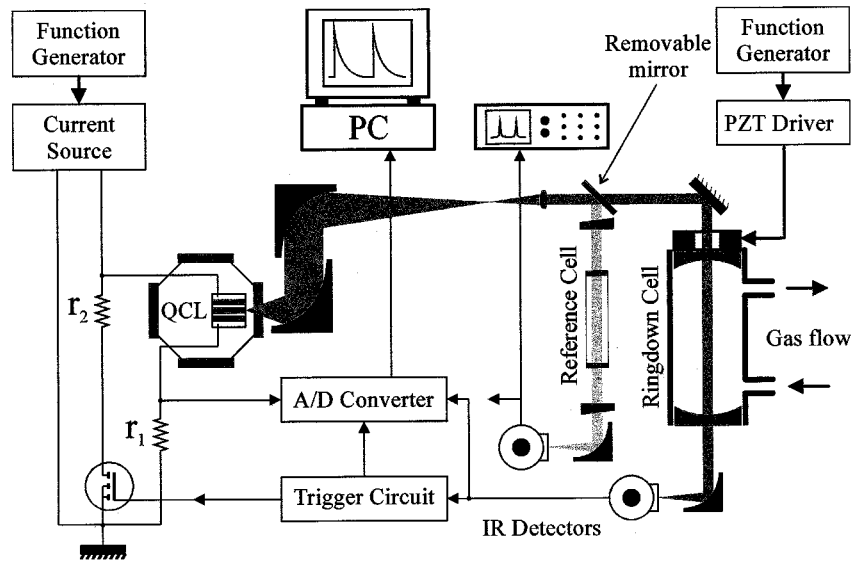


Fig. 7. Schematic of a CRDS-based gas sensor [14]. r_1 : current monitor resistor; r_2 : current-limiting resistor. Two wedged ZnSe windows shown near the reference cell were used to form an etalon for fine frequency calibration.

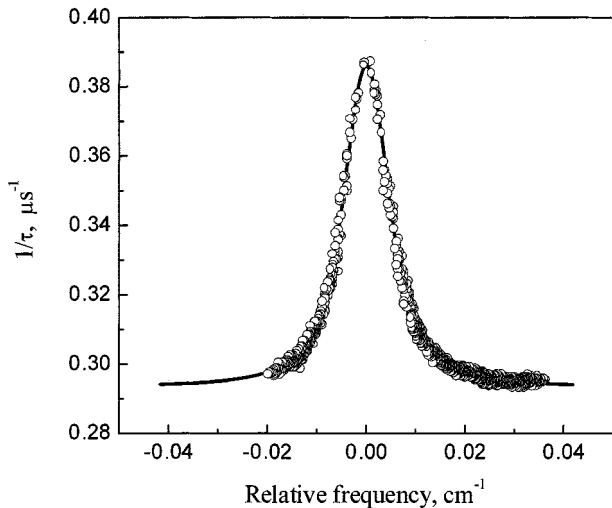


Fig. 8. CRDS spectrum of NO in N_2 , unresolved lines at 1921.599 cm^{-1} and 1921.601 cm^{-1} . The solid line shows a Voigt fit, which resulted in NO concentration of 622 ppbv.

pure N_2 is presented in Fig. 8. A noise-equivalent sensitivity was estimated to be 0.7 ppbv for an 8-s data acquisition time. It was not possible to use this sensor directly for measurements of NO concentration in exhaled air (~ 10 ppbv) because of a strong CO_2 interference, which can be avoided if the appropriate NO absorption line is chosen (such as the R(7.5) components at 1903.123 and 1903.134 cm^{-1}).

B. Cavity Enhanced Absorption Spectroscopy

A simpler (as compared to CRDS) way to exploit a high-finesse optical cavity for increasing the sensitivity to absorption was suggested in [36] and [37] published in 1998. Essentially the same technique was called “integrated cavity output spectroscopy” (ICOS) in [36] and “cavity enhanced absorption” (CEA) in [37]. This method consists of detecting the time-integrated signal upon exiting the high-finesse optical cavity, averaged over many cavity modes and corresponds to the schematic

in Fig. 6(a). The condition $\Delta\nu_L \gg \Omega$ can be satisfied with either a broad-band pulsed laser source or by dithering of one of the cavity mirrors to generate random jittering of the cavity modes. In [37], the authors also used the geometry involving many transversal cavity modes in order to achieve a denser cavity transmission spectrum. It can be shown that the output signal I in case of perfect spatial coupling is given by

$$I = I_0 \frac{(1-R)^2}{2[(1-R) + \alpha l]} \quad (3)$$

where I_0 is the laser intensity. For weak absorption $\alpha l \ll 1-R$, this equation converts to

$$\frac{I}{I_0} \approx \frac{1-R}{2} \left(1 - \frac{\alpha l}{1-R} \right) \quad (4)$$

yielding the same effective pathlength of $L = l/(1-R)$ as CRDS. Hence, the absorption measurements are performed in essentially the same way as with a conventional multipass cell, except that the ICOS signal does not decrease exponentially with αl .

The described approach that we shall refer to as CES was demonstrated with a CW QC-DFB laser in [38]. The laser operated at $\lambda = 5.2\ \mu\text{m}$ with a maximum output power of 80 mW. This particular CES sensor was designed for NO detection in human breath samples. A direct performance comparison was carried out between a sensor configuration where the optical cavity was replaced with a 100-m pathlength multipass cell. It was found that, regardless of the effective pathlength of $L = 670\text{ m}$, CES spectra resulted in a lower absorption sensitivity because of baseline noise of $\sim 1\%$ (averaging 10^4 QC laser scans). These baseline fluctuations are intrinsic to CES and result from the mode structure of the cavity transmission spectrum. In a single laser scan the quasirandom intensity fluctuations are $\sim 100\%$ [Fig. 9(a)]. The averaging of N scans with cavity mirror dithering results in a decrease of the fluctuation magnitude that is inversely proportional to $N^{1/2}$ [Fig. 9(b)]. This yields a minimum detectable $1\% I/I_0$ variation of 1% with

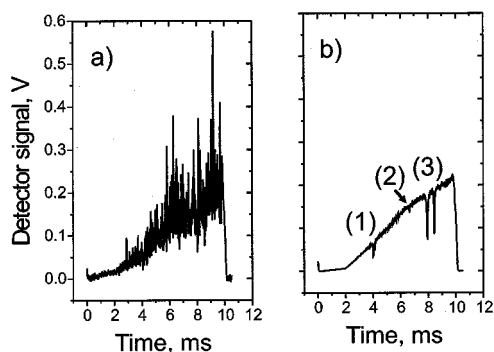


Fig. 9. Transmitted intensity through the high-finesse optical cavity filled with 50 torr of ambient air [38] for (a) a single scan and (b) 10^3 averaged scans. A linear current ramp for frequency scanning was applied to the QC-DFB laser. Observed absorption lines were: (1): H₂O at ~ 1920.9 cm⁻¹, (2): CO₂ at 1920.1 cm⁻¹, (3): H₂O at 1919.7 cm⁻¹ and 1919.5 cm⁻¹.

the longest practical averaging of 10^4 scans. Therefore, in our studies to date, we find that CES appears to be a less sensitive technique than CRDS. However, experimentally CES is simpler, can realize a higher dynamic range [38], and is certainly effective in applications that require moderately sensitive, compact chemical sensors based on QC-DFB lasers. Some improvement in a CES baseline noise can be achieved with a recently developed off-axis technique [39].

IV. PHOTOACOUSTIC TRACE GAS DETECTION

Photoacoustic spectroscopy (PAS), based on the photoacoustic effect, in which acoustic waves result from the absorption of laser radiation by a selected target compound in a specially designed cell is another effective method for sensitive trace gas detection. In contrast to other mid-IR absorption techniques, PAS is an indirect technique in which the effect on the absorbing medium and not the direct light absorption is detected. Light absorption results in a transient temperature effect, which then translates into kinetic energy or pressure variations in the absorbing medium via nonradiative relaxation processes, which can be detected with a sensitive microphone. There are two modes of operation for PAS; either the exciting light can be modulated at a frequency away from any cell resonance or adjusted to coincide with an acoustic resonant frequency. The in-resonance mode is usually employed with the low-power pump lasers. PAS is ideally a background-free technique, since the signal is generated by the absorbing gas. In real PAS experiments, background signals can originate from nonselective absorption of the gas cell windows (coherent noise) and an outside acoustic (incoherent) noise. PAS signals are proportional to the pump laser intensity and therefore PAS has mostly used high-power laser sources. However, a sensitivity of 8 ppmv was demonstrated with only 2 mW of modulated diode laser power in the CH₄ overtone region [40]. An implementation of a QC-DFB laser in the fundamental absorption region has a potential of considerably improved sensitivity.

Ammonia and water vapor photoacoustic spectra were obtained using a CW cryogenically cooled QC-DFB laser with a 16-mW power output at 8.5 μ m as reported in [41]. A PAS cell resonant at 1.66 kHz was used. The QC-DFB was frequency scanned using temperature tuning, and for real-time concentration measurements the laser temperature was fixed to measure

absorption at a certain wavelength. Measured concentrations ranged from 2200 ppmv to 100 ppbv. The laser beam was modulated by use of a mechanical chopper with a 50% duty cycle. The microphone PAS signal was processed by a lock-in amplifier and normalized with the intensity measured by a HgCdTe detector. The mode stability was monitored by a ZnSe Fabry-Pérot etalon (5-cm-long, 3-GHz free spectral range). A detection limit of 100 ppbv ammonia ($\sim 10^{-5}$ noise-equivalent absorbance) at standard temperature and pressure was obtained for a 1-Hz bandwidth and a measurement interval of 10 min. Hence, the sensitivity obtained is comparable with that achieved by the direct absorption techniques described in Sections II-IV, but the required scan times are longer for PAS.

Recently, Hofstetter *et al.* [42], [43] reported PAS measurements of ammonia, methanol, and carbon dioxide using a pulsed QC-DFB laser operated at 3%–4% duty cycle with 25-ns-long current pulses (2-mW average power) and operation close to room temperature with Peltier cooling. Temperature tuning resulted in a wavelength range of 3 cm⁻¹ at a linewidth of 0.2 cm⁻¹. This sensor used a 42-cm-long PAS cell with a radial 16-microphone array for increased detection sensitivity. In addition, the cell was placed between two concave reflectors resulting in 36 passes through the cell (with an effective pathlength of 15 m). The laser beam was mechanically chopped at a resonant cell frequency of 1.25 kHz, which resulted in PAS signal enhancement by a Q factor of 70. A pyroelectric detector recorded the QC laser power to normalize the PAS signal. Detection of ammonia concentrations at the 300 ppbv level with a SNR of 3 was achieved at a pressure of 400 mbar.

V. NONLINEAR SPECTROSCOPY WITH QC-DFB LASERS

High power and the potentially narrow spectral linewidth of QC lasers open up the possibility to use these devices in nonlinear laser spectroscopy. The first experimental demonstration of nonlinear light-matter interaction involving a QC-DFB laser² as a light source was reported in [44]. In this paper it was demonstrated that a free-running QC-DFB laser operated in a rapid scan mode has sufficient beam quality, power, and linewidth to produce sub-Doppler saturation features in a simple Lamb-dip geometry. A 30-mW laser beam was focused into the cell using a 150-mm focal length lens, and a Lamb dip was observed in absorption spectra of <20 mtorr NO gas. The observed Lamb dip width was limited by the laser linewidth to 4.3 MHz, which is a factor of 30 below the Doppler limit.

There is an even greater potential to exploit nonlinear laser spectroscopic methods if the QC laser is locked to a high-finesse optical cavity. The intensity of the resonant laser field is increased in an empty cavity formed by two lossless dielectric mirrors $1/(1-R)$ times, where R is the reflection coefficient of each mirror. We can assume laser and mirror parameters from [14], namely that the laser power $I_0 = 20$ mW, $\Delta\nu_L = 3$ MHz, $R = 99.965\%$, and suppose a mirror spacing $l = 20$ cm. The cavity mode width $\Delta\nu_C = c(1-R)/2\pi l \approx 84$ kHz, and the resonant fraction of the laser radiation is $T \approx \Delta\nu_C/\Delta\nu_L = 0.03$ (this fraction can be increased with smaller

²Another example of the nonlinear interaction is passive modelocking of QC lasers [4], but this effect occurs inside the laser medium and is beyond the scope of this review.

mirror separation; perfect spatial coupling is assumed). With these assumptions, the intracavity power can be estimated to be $I_C = TI_0/(1 - R) = 1.7$ W. This power can be focused inside the cavity by the proper choice of the cavity geometry and provide an adequate power density level for various nonlinear optical effects. An observation of a cavity-enhanced Lamb-dip measurement using a QC laser was demonstrated in [33].

VI. CONCLUSION

Compact, sensitive, and selective gas sensors based on mid-infrared CW and pulsed QC-DFB lasers have been demonstrated to be potentially capable of numerous applications since 1998. These include such diverse fields as environmental monitoring (atmospheric chemistry, CO, CO₂, CH₄, and H₂CO are important in global warming and ozone depletion studies, volcanic plume emissions), industrial emission measurements (e.g., fence line perimeter monitoring in the petrochemical industry, combustion sites, waste incinerators, down gas well monitoring, gas-pipe and compressor station safety), urban (e.g., automobile traffic, power generation,) and rural emissions (e.g., horticultural greenhouses, fruit storage, and rice agro-ecosystems), chemical analysis and control for manufacturing processes (e.g., semiconductor, pharmaceutical, food), detection of medically important molecules (e.g., NO, CO, CO₂, NH₃, C₂H₆ and CS₂), toxic gases, drugs, and explosives relevant to law enforcement and public safety, and spacecraft habitat air-quality and planetary atmospheric science (e.g., such planetary gases as H₂O, CH₄, CO, CO₂ and C₂H₂).

To date, QC laser-based chemical sensors primarily use InGaAs/InAlAs type-I QC-DFB devices. There are two limitations inherent to this kind of lasers for chemical sensing. First, they cannot access the spectral region of C-H and O-H stretch vibrations near 3000 cm⁻¹. This shortcoming can be overcome by developing QC lasers based on alternative materials and structures. For example, the 3000-cm⁻¹ region is accessible by type-II lasers [6], [7], but no single-frequency devices of this kind are available. Another issue is the limited tunability of each QC-DFB laser, which restricts the feasibility of multi-component chemical sensing. This requirement can be addressed by separating the gain medium from the wavelength-selective element. In [45], a QC laser tunability of ~35 cm⁻¹ at a fixed temperature was demonstrated in an external cavity configuration with a diffraction grating. This is about a ten times wider range than that the typically achieved for QC-DFB lasers by means of current tuning. Recently an ultrabroad-band laser medium based on a number of combined dissimilar intersubband optical transitions was reported [46]. This medium provided an optical gain from 5 to 8 μm, which corresponds to a 750-cm⁻¹ bandwidth.

Progress to date in terms of performance optimization of various CW and pulsed single-frequency QC-DFB laser sources, different sensitivity enhancement schemes, and minimum detectable absorbances (10⁻⁴ to 10⁻⁶) limited by laser, optical, and detector noise sources by several research groups, including the one of the authors have been described. On-line, autonomous concentration measurements of ~20 gaseous compounds and several isotopomers in ambient air have been realized in the first three years of QC laser-based chemical sensors.

ACKNOWLEDGMENT

The authors thank Dr. R. F. Curl for numerous useful discussions and support of this work. They are also grateful to Dr. C. Gmachl and Dr. F. Capasso for their invaluable scientific and technical support.

REFERENCES

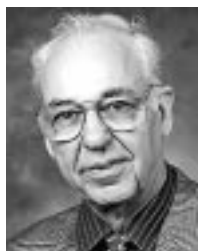
- [1] A. Fried, B. Henry, B. Wert, S. Sewell, and J. R. Drumming, "Laboratory, ground-based, and airborne tunable diode laser systems: Performance characteristics and applications in atmospheric studies," *Appl. Phys. B*, vol. 67, pp. 317–330, 1998.
- [2] C. E. Kolb, J. C. Wormhoudt, and M. S. Zahniser, "Recent advances in spectroscopic instrumentation for measuring stable gases in the natural environment," in *Methods in Ecology: Biogenic Trace Gases: Measuring Emissions From Soil and Water*, P. A. Matson and R. C. Harriss, Eds. Edinburgh, U.K.: Blackwell Scientific, 1995, pp. 259–290.
- [3] D. Richter, D. G. Lancaster, and F. K. Tittel, "Development of an automated diode laser based multi-component gas sensor," *Appl. Opt.*, vol. 39, pp. 4444–4450, 2000.
- [4] F. Capasso, C. Gmachl, R. Paiella, A. Tredicucci, A. L. Hutchinson, D. L. Sivco, J. N. Baillargeon, and A. Y. Cho, "New frontiers in quantum cascade lasers and applications," *IEEE Select. Topics Quantum Electron.*, vol. 6, pp. 931–947, 2000.
- [5] L. Hvozdar, S. Gianordoli, G. Strasser, W. Schrenk, K. Unterrainer, E. Gornik, C. S. S. Murthy, M. Kraft, V. Pustogov, B. Mizaikoff, A. Inberg, and N. Croitoru, "Spectroscopy in the gas phase with GaAs/Al-GaAs quantum-cascade lasers," *Appl. Opt.*, vol. 39, pp. 6926–6930, 2000.
- [6] R. Q. Yang, C.-H. Lin, B. H. Yang, D. Zhang, S. J. Murry, S. S. Pei, W. W. Bewley, L. J. Olafsen, E. H. Aifer, C. L. Felix, I. Vurgaftman, and J. R. Meyer, "Type-II quantum cascade lasers," in *Proc. SPIE*, vol. 3284, 1998, pp. 308–317.
- [7] W.-Y. Hwang, S. V. Zaitsev, C. H. Kuo, H.-L. Chih, J. Um, A. Delaney, Z. Jun, S. J. Murry, and A. Liu, "High-performance mid-IR type-II interband cascade lasers," in *Conf. Lasers and Electro-Optics, OSA Tech. Dig.* Washington, DC, 2000, pp. 59–62.
- [8] D. Hofstetter, M. Beck, T. Aellen, and J. Faist, "High temperature operation of distributed feedback quantum-cascade lasers at 5.3 μm," *Appl. Phys. Lett.*, vol. 78, pp. 396–398, 2001.
- [9] A. O'Keefe and D. A. G. Deacon, "Cavity ring-down optical spectrometer for absorption measurements using pulsed laser sources," *Rev. Sci. Instrum.*, vol. 59, pp. 2544–2551, 1988.
- [10] G. Berden, R. Peeters, and G. Meijer, "Cavity ring-down spectroscopy: Experimental schemes and applications," *Int. Rev. Phys. Chem.*, vol. 19, pp. 565–607, 2000.
- [11] D. Hofstetter, M. Beck, T. Aellen, J. Faist, U. Oesterle, M. Ilegems, E. Gini, and H. Melchior, "Continuous wave operation of a 9.3 μm quantum cascade laser on a Peltier coolant," *Appl. Phys. Lett.*, vol. 78, pp. 1964–1966, 2001.
- [12] M. Beck, D. Hofstetter, T. Aellen, J. Faist, U. Oesterle, M. Ilegems, E. Gini, and H. Melchior, "Continuous wave operation of a mid-infrared semiconductor laser at room temperature," *Science*, vol. 295, pp. 301–305, 2002.
- [13] C. R. Webster, G. J. Flesch, D. C. Scott, J. E. Swanson, R. D. May, W. S. Woodward, C. Gmachl, F. Capasso, D. L. Sivco, J. N. Baillargeon, A. L. Hutchinson, and A. Y. Cho, "Quantum-cascade laser measurements of stratospheric methane and nitrous oxide," *Appl. Opt.*, vol. 40, pp. 321–326, 2001.
- [14] A. A. Kosterev, A. A. Malinovsky, F. K. Tittel, C. Gmachl, F. Capasso, D. L. Sivco, J. N. Baillargeon, A. L. Hutchinson, and A. Y. Cho, "Cavity ringdown spectroscopic detection of nitric oxide with a continuous-wave quantum-cascade laser," *Appl. Opt.*, vol. 40, pp. 5522–5529, 2001.
- [15] T. L. Myers, R. M. Williams, M. S. Taubman, F. Capasso, C. Gmachl, D. L. Sivco, J. N. Baillargeon, and A. Y. Cho, "Free-running frequency stability of mid-infrared quantum cascade lasers," *Opt. Lett.*, vol. 27, pp. 170–172, 2002.
- [16] H. Ganser, B. Frech, A. Jentsch, M. Muertz, C. Gmachl, F. Capasso, D. L. Sivco, J. N. Baillargeon, A. L. Hutchinson, A. Y. Cho, and W. Urban, "Investigation of the spectral width of quantum cascade laser emission near 5.2 μm by a heterodyne experiment," *Opt. Commun.*, vol. 197, pp. 127–130, 2001.
- [17] R. M. Williams, J. F. Kelly, and J. S. Hartman *et al.*, "Kilo-hertz linewidth from frequency stabilized mid infrared quantum cascade lasers," *Opt. Lett.*, vol. 24, pp. 1844–1846, 1999.

- [18] S. W. Sharpe, J. F. Kelly, J. S. Hartman, C. Gmachl, F. Capasso, D. L. Sivco, J. N. Baillargeon, and A. Y. Cho, "High-resolution (Doppler-limited) spectroscopy using quantum-cascade distributed-feedback lasers," *Opt. Lett.*, vol. 23, pp. 1396–1398, 1998.
- [19] A. A. Kosterev, R. F. Curl, F. K. Tittel, C. Gmachl, F. Capasso, D. L. Sivco, J. N. Baillargeon, A. L. Hutchinson, and A. Y. Cho, "Methane concentration and isotopic composition measurements with a mid-infrared quantum cascade laser," *Opt. Lett.*, vol. 24, pp. 1762–1764, 1999.
- [20] —, "Effective utilization of quantum-cascade distributed-feedback lasers in absorption spectroscopy," *Appl. Opt.*, vol. 39, pp. 4425–4430, 2000.
- [21] A. Fried, S. Sewell, B. Henry, B. P. Wert, T. Gilpin, and J. R. Drummond, "Tunable diode laser absorption spectrometer for ground-based measurements of formaldehyde," *J. Geophys. Res.*, vol. 102, pp. 6253–6266, 1997.
- [22] R. Koehler, C. Gmachl, F. Capasso, A. Tredicucci, D. L. Sivco, and A. Y. Cho, "Single-mode tunable quantum cascade lasers in the spectral range of the CO₂ laser at $\lambda = 9.5\text{--}10.5\ \mu\text{m}$," *IEEE Photon. Technol. Lett.*, vol. 12, pp. 474–476, 2000.
- [23] C. M. Gittins, E. T. Wetjen, C. Gmachl, F. Capasso, A. L. Hutchinson, D. L. Sivco, J. N. Baillargeon, and A. Y. Cho, "Quantitative gas sensing by backscatter-absorption measurements of a pseudorandom code modulated $\lambda \sim 8\text{-}\mu\text{m}$ quantum cascade laser," *Opt. Lett.*, vol. 25, pp. 1162–1164, 2000.
- [24] K. Namjou, S. Cai, E. A. Whittaker, J. Faist, C. Gmachl, F. Capasso, D. L. Sivco, and A. Y. Cho, "Sensitive absorption spectroscopy with a room-temperature distributed-feedback quantum-cascade laser," *Opt. Lett.*, vol. 23, pp. 219–221, 1998.
- [25] D. M. Sonnenfroh, W. T. Rawlins, M. G. Allen, C. Gmachl, F. Capasso, A. L. Hutchinson, D. L. Sivco, J. N. Baillargeon, and A. Y. Cho, "Application of balanced detection to absorption measurements of trace gases with room-temperature, quasicW quantum-cascade lasers," *Appl. Opt.*, vol. 40, pp. 812–820, 2000.
- [26] A. A. Kosterev, F. K. Tittel, C. Gmachl, F. Capasso, D. L. Sivco, J. N. Baillargeon, A. L. Hutchinson, and A. Y. Cho, "Trace gas detection in ambient air with a thermoelectrically cooled QC-DFB laser," *Appl. Opt.*, vol. 39, pp. 6866–6872, 2000.
- [27] A. A. Kosterev, R. F. Curl, F. K. Tittel, R. Köhler, C. Gmachl, F. Capasso, D. L. Sivco, and A. Y. Cho, "Transportable automated ammonia sensor based on a pulsed thermoelectrically cooled QC-DFB laser," *Appl. Opt.*, vol. 41, pp. 573–578, 2002.
- [28] A. A. Kosterev, F. K. Tittel, R. Köhler, C. Gmachl, F. Capasso, D. L. Sivco, A. Y. Cho, S. Wehe, and M. G. Allen, "Thermoelectrically cooled quantum cascade laser based sensor for continuous monitoring of ambient atmospheric CO," *Appl. Opt.*, vol. 41, pp. 1169–1173, 2002.
- [29] A. A. Kosterev, F. K. Tittel, W. Durante, M. G. Allen, R. Köhler, C. Gmachl, F. Capasso, D. L. Sivco, and A. Y. Cho, "Detection of biogenic CO production above vascular cell cultures using a near-room temperature QC-DFB laser," *Appl. Phys. B*, vol. 74, pp. 95–99, 2002.
- [30] Y. Morimoto, W. Durante, D. G. Lancaster, J. Klattenhoff, and F. K. Tittel, "Real-time measurements of endogenous CO production from vascular cells using an ultrasensitive laser sensor," *Amwe. J. Physiol. Heart Circ. Physiol.*, vol. 280, pp. H483–H488, 2001.
- [31] B. Lendl, J. Frank, R. Schindler, A. Müller, M. Beck, and J. Faist, "Mid-infrared quantum cascade lasers for flow injection analysis," *Anal. Chem.*, vol. 72, pp. 1645–1648, 2000.
- [32] J. Ye, L.-S. Ma, and J. L. Hall, "Sub-doppler optical frequency reference at 1.064 μm by means of ultrasensitive cavity-enhanced frequency modulation spectroscopy of a C₂H_d overtone transition," *Opt. Lett.*, vol. 21, pp. 1000–1002, 1996.
- [33] M. S. Taubman, R. M. Williams, T. L. Myers, F. Capasso, C. Gmachl, D. L. Sivco, A. L. Hutchinson, and A. Y. Cho, "Sub-Doppler NICE-OHMS spectroscopy at 8.5 microns using a quantum cascade laser," in *Proc. Conf. Lasers and Electro-Optics (CLEO 2002)*, Long Beach, CA, May 19–24, 2002.
- [34] D. Romanini, A. A. Kachanov, N. Sadeghi, and F. Stoekel, "CW cavity ring down spectroscopy," *Chem. Phys. Lett.*, vol. 264, pp. 316–322, 1997.
- [35] B. A. Paldus, C. C. Harb, T. G. Spence, R. N. Zare, C. Gmachl, F. Capasso, D. L. Sivco, J. N. Baillargeon, A. L. Hutchinson, and A. Y. Cho, "Cavity ringdown spectroscopy using mid-infrared quantum-cascade lasers," *Opt. Lett.*, vol. 25, pp. 666–668, 2000.
- [36] A. O'Keefe, "Integrated cavity output analysis of ultra-weak absorption," *Chem. Phys. Lett.*, vol. 293, pp. 331–336, 1998.
- [37] R. Engeln, G. Berden, R. Peeters, and G. Meijer, "Cavity enhanced absorption and cavity enhanced magnetic rotation spectroscopy," *Rev. Sci. Instrum.*, vol. 69, pp. 3763–3769, 1998.
- [38] L. Menzel, A. A. Kosterev, R. F. Curl, and F. K. Tittel, "Spectroscopic detection of biological NO with a quantum cascade laser," *Appl. Phys. B*, vol. 72, pp. 859–863, 2001.
- [39] J. B. Paul, L. Lapson, and G. Anderson, "Ultrasensitive absorption spectroscopy with a high-finesse optical cavity and off-axis alignment," *Appl. Opt.*, vol. 40, pp. 4904–4910, 2001.
- [40] G.-C. Liang, H.-H. Liu, A. H. Kung, A. Mohacsi, A. Miklos, and P. Hess, "Photoacoustic trace detection of methane using compact solid-state lasers," *J. Phys. Chem. A*, vol. 104, pp. 10 179–10 183, 2000.
- [41] B. A. Paldus, T. G. Spence, R. N. Zare, J. Oomens, F. J. M. Harren, D. H. Parker, C. Gmachl, F. Capasso, D. L. Sivco, J. N. Baillargeon, A. L. Hutchinson, and A. Y. Cho, "Photoacoustic spectroscopy using quantum-cascade lasers," *Opt. Lett.*, vol. 24, pp. 178–180, 1999.
- [42] D. Hofstetter, M. Beck, J. Faist, M. Naegel, and M. W. Sigrist, "Photoacoustic spectroscopy with quantum cascade distributed-feedback lasers," *Opt. Lett.*, vol. 26, pp. 887–889, 2001.
- [43] M. Nägele, D. Hofstetter, J. Faist, and M. W. Sigrist, "Low power quantum-cascade laser photoacoustic spectrometer for trace-gas monitoring," *Analytic. Sci.*, vol. 17, pp. s497–s499, 2001.
- [44] J. T. Remillard, D. Uy, W. H. Weber, F. Capasso, C. Gmachl, A. L. Hutchinson, D. L. Sivco, J. N. Baillargeon, and A. Y. Cho, "Sub-doppler resolution limited lamb-dip spectroscopy of NO with a quantum cascade distributed feedback laser," *Opt. Express*, vol. 7, pp. 243–248, 2000.
- [45] G. P. Luo, C. Peng, H. Q. Le, S. S. Pei, W.-Y. Hwang, B. Ishaug, J. Um, J. N. Baillargeon, and C.-H. Lin, "Grating-tuned external-cavity quantum-cascade semiconductor lasers," *Appl. Phys. Lett.*, vol. 78, pp. 2834–2836, 2001.
- [46] C. Gmachl, D. L. Sivco, R. Colombelli, F. Capasso, and A. Y. Cho, "Ultra-broadband semiconductor laser," *Nature*, vol. 415, pp. 883–887, 2002.



Anatoliy A. Kosterev was born in Voronezh Region, Russia, in 1962. He received the M.Sc. degree in physics from the Moscow Institute of Physics and Technology in 1985 and the Ph.D. degree in physics from the Institute of Spectroscopy, Russian Academy of Sciences, in 1995, based on his investigations in the field of vibrational molecular dynamics.

In 1998, he joined the Laser Science Group of Rice University, Houston, TX, where his current research interests are directed to chemical sensing applications of quantum cascade lasers.



Frank K. Tittel (SM'72–F'86) was born in Berlin, Germany, in 1933. He received the B.S., M.S., and Ph.D. degrees in physics from the University of Oxford, Oxford, U.K., in 1955 and 1959, respectively.

From 1959 to 1967, he was a Research Physicist with General Electric (GE) Research and Development Center, Schenectady, NY. At GE, he carried out early pioneering studies of dye lasers and high power solid state lasers. Since 1967, he has been on the faculty of the Department of Electrical and Computer Engineering at Rice University in Houston, TX, where is currently an Endowed Chair Professor. In 1973 and 1981, he was an Alexander von Humboldt Senior Fellow at the Max-Planck Institutes of Biophysical Chemistry, Göttingen, and Quantum Optics, Munich, respectively. He held visiting professor appointments at NASA Goddard Space Flight Center, University of Aix-Marseille, Keio University (Japan), and Swiss Institute of Technology (ETH-Zurich). Current research interests include various aspects of quantum electronics, in particular laser spectroscopy, nonlinear optics, and laser applications in environmental monitoring, process control, and medicine. He has published more than 300 technical papers and holds seven U.S. patents in these areas.

Dr. Tittel is a Fellow of the Optical Society of America (OSA) and the American Physical Society (APS). He received a Doctor of Science (HC) degree from JATE University, Szeged, Hungary, in 1993. He is an Associate Editor of *Applied Physics B*, and a former Editor-in-Chief of *IEEE JOURNAL OF SELECTED TOPICS IN QUANTUM ELECTRONICS* (1996–1998) and Associate Editor of the *IEEE JOURNAL OF QUANTUM ELECTRONICS*. He has served on numerous technical program committees such as CLEO, IQEC, and QELS for OSA and APS.